ROLE OF INTERNAL HE AT SOURCE FOR ERUPTI VE PLUMES ON TRITON

N. s. Duxbury

R. 11. Brown

Corresponding author: N. S. Duxbury

M. S. 183 501,

Jet Propulsion Laborat ory,

4s00 OakGrove 1)1'.,

Pasadena, CA 91109

t el. 818 354 55 16

e-mail nsd@scn1.jpl.nasa.gov

Key W()]'(is: Triton, nitrogen, plumes, internal. subsurface

Running title: Tritonian eruptions

For the first time the role of the internal heat source, due to radioactive decay in Triton's core, is investigated with respect to geyser-like plumes. Triton is one of only three known objects in the Solar System (the other two are Earth and the Jovian satellite Io) where eruptive activity has been definitely observed. A new mechanism of energy supply to the Tritonian eruptive plumes is proposed. This mechanism is based on heat transport in the solid-nitrogen polar caps due to thermal convection, in addition to conduction. The conductive-convective model shows that a 1 K increase in the N_2 ice subsurface temperature over the surface value is reached much closer to the surface in a region of upwelling subsurface plume compared to a pure conductive case. This temperature rise is sufficient to double the nitrogen vapor pressure. Therefore, it is enough to drive the atmospheric plumes to the observed height of ≈ 8 km, provided 1 K warmer nitrogen ice encounters a vent and hence is exposed to the ≈ 15 μbar Tritonian atmosphere. Solid-state convection onsets if a nitrogen layer is sufficiently thick and the average solid N_2 grain size is small enough. We present the critical values of these parameters for Triton. A possible origin of the subsurface vents on Triton is also suggested.

N. Ibbetson and R. Brown

INTRODUCTION

The discovery of 8-km-high, geyser-like plumes in images of Neptune's largest satellite Triton was a highlight of the Voyager 2 mission (Smith *et al.* 1989). At least four active geyser-like plumes were observed using stereo imaging shortly after the Voyager 2 flyby in August 1989 (Soderblom *et al.* 1990). Stereo imaging helped to distinguish between the albedo markings and above-the-surface phenomena. Eruptions at 49 S, 2 E and 57 S, 38 E were documented quite well. They were dark columns of gas and dust, with radii up to about 1 km, which were driven downwind over 100 km after reaching a height of about 8 km. Their lifetime was estimated to be on the order of one to five Earth years. This phenomenon is surprising at first glance because Triton is far from the Sun (≈30 A.U.) and its surface temperature of ≈38 K is one of the lowest in the Solar System. In fact, it is much lower than was expected before the Voyager flyby, when some investigators were considering a liquid nitrogen ocean on Triton's surface.

During the Voyager 2 encounter it was spring in Triton's Southern Hemisphere, with the subsolar point at 45 S and moving farther south to its extreme position of 52 S. Since the geyser-like plumes were identified on Triton only in areas of continuous sunlight, solar energy was thought to play an important role in driving these phenomena. Brown *et al.* (1990) investigated solid-state greenhouses as mechanisms of solar energy supply to the plumes. Here we evaluate the plausibility of an alternative heat source: internal heat due to radioactive decay in Triton's inferred silicate core. We also investigate an alternative mechanism of energy supply: convection in the solid nitrogen caps.

The previous models of seasonal volatile transport on Triton (Spencer 1990, Spencer and Moore 1992, Hansen and Paige 1992) considered only conductive heat transfer. Using an analogy with water-ice glaciers on Earth, viscous flow was incorporated for the first time in the model of Brown and Kirk (1994) without considering convective effects. In their work only the along slope velocity was calculated for estimating solar cap spreading - the non-linear convective term $\nabla T \bullet V$ was not included.

PHYSICAL MODEL

Following Smith *et al.* (1989), we consider Triton to be completely differentiated into

a rocky core, a water-ice mantle and a surface layer of volatile ices. The ground-based discovery of nitrogen on the Triton's surface by Cruikshank *et al.* (1984) was confirmed by the identification of a primarily nitrogen atmosphere during the Voyager 2 flyby. From recent ground-based spectroscopy (Cruikshank *et al.* 1993) it is known that solid nitrogen comprises $\approx 99\%$ of Triton's surface ices, being at least tens of centimeters deep (since the nitrogen absorption feature is usually so weak that its identification speaks for the presence of a deep N_2 layer). Therefore, in our basic model we assume pure nitrogen polar caps. Permanent solid N_2 layers are considered to be bright (Duxbury and Brown 1993), and seasonally formed nitrogen ice to be transparent (Eluszkiewicz 1991). Nitrogen is highly volatile at Triton's temperatures and is believed to be in vapor pressure equilibrium with the atmosphere. (Note that N_2 vapor pressure is very sensitive to temperature changes.) Hence, due to latent heat of sublimation-condensation effects, the satellite has a nearly isothermal icy surface, when even the temperature of N_2 ice on the dark side of Triton is the same as on the day side. The temperature of the lower atmosphere was measured by Voyager 2 as 38^{+3}_{-4} K, and from more recent ground-based spectroscopy the surface temperature was obtained (Tryka *et al.* 1993, 1994) more precisely as 38^{+1}_{-1} K.

An extensive silicate core has been inferred for Triton (Smith *et al.* 1989) from a relatively high mean density of 2.054 g/cm^3 (Voyager 2 estimate). The core radius was estimated to be $\approx$1000 km, whereas Triton's mean radius is about 1352 km. Hence the core comprises $\approx$70 % of Triton's mass. It was estimated by Brown *et al.* (1991) that the internal heat source can amount to 5 - 20% of Triton's absorbed insolation. Whence Triton's internal heat source due to the radioactive decay in the core is the largest, in proportion to the insolation it absorbs, among all outer planet satellites, except Io. These clues and the preliminary estimates of the Rayleigh numbers for solid nitrogen at plausible values for Triton's subsurface temperatures, suggest that solid-state convection in nitrogen polar caps, as an alternative mechanism, could supply the energy necessary to drive the plumes from the internal heat flow.

Here we consider conductive heat transfer and convective heat and mass transport in the subsurface due to the permanent basal heating of the solid nitrogen layer. A significant temperature increase at the base of the solid nitrogen layer is caused by the large

thermal conductivity differences of the water-ice mantle and the overlying nitrogen ice. Using laboratory measurements (Klinger 1980) of the water-ice thermal conductivity gives: $\lambda_{H_2O}/\lambda_{N_2} \approx 50\text{-}100$ in the range of temperatures 40-63 K plausible at the nitrogen ice - mantle interface. Consequently, solid nitrogen acts as a thermal insulator for the mantle from the outer cooling. From the condition of energy conservation on the boundary between nitrogen ice and water ice, and from the estimate of ≈0.3 K/km for the steady-state temperature gradient in H_2O ice by Smith *et al.* (1989), the gradient in the nitrogen layer is ≈15 - 30 K/km. Convection in solid N_2 redistributes a uniform basal heat flow in a way that the surface heat flow is significantly increased in the vicinity of an upwelling plume. We will be interested in the locations of 39 K isotherms, since there (under the assumption of a 38 K surface temperature) the difference of 1 K is reached, which is sufficient to double N_2 vapor pressure.

Following Kirk (1990), we consider that at low stress levels (resulting from a relatively small thickness of nitrogen layers and small slopes) and at Triton's temperatures, DIFFUSION CREEP is the dominant solid-state creep mechanism. Thus we treat nitrogen ice as a Newtonian viscous fluid with a shear viscosity independent of stress. We are not interested in bulk viscosity, since it is multiplied by energy dissipation due to compression, and in the Boussinesq approximation density is considered constant everywhere except in the buoyancy term.

Dislocation creep (which is alternative to the diffusion creep) is described by a non-linear flow law, leading to the viscosity being dependent not only upon temperature and pressure, but on stress as well. However, even in the case of the Earth's mantle many model calculations show (see Schubert 1979 pp. 297-298 for ref.) that choosing of either a linear or non-linear flow law is not essential. Both mechanisms are thermally activated and therefore have the same exponential form of dependence of effective viscosity upon temperature and pressure (see Christensen 1984 for formulas). The dependence of viscosity upon these parameters far outweighs its dependence upon stress, i.e. it is much more important than the influence of a nonlinear relation between stress and strain rate. The insignificant influence of stress upon viscosity compared to the temperature and pressure influence in power-law creep was also recently shown in the experiments of Goldsby and Kohlstedt

(1995). They performed measurements for H_2O ice I under low stresses (Goldsby, pers. communications, 1995). Therefore, we are concerned here only with Newtonian rheology. For the range of thicknesses we consider, it is also possible to neglect the dependence of viscosity upon pressure since the pressure at the base of 1-km N_2 layer is only about 7.9 bar.

We model conductive-convective heat and mass transport in Triton's nitrogen cap for a two dimensional, steady-state case in the permanent deposits up to 1.2 km thick, considering thermal convection with heating only from below (i.e. Rayleigh-Benard case). On the upper boundary the tangential component of the shear stress is taken as zero. All modeling is performed here for the case when the basal temperature (63 K) is lower than the nitrogen melting temperature (63.148 K at P= 0). Unlike water ice, solid N_2 does not undergo pressure induced melting. Hence thickening of a cap does not reduce the nitrogen melting temperature and does not produce melt at the base. On the contrary, the melting temperature increases with presure growth (Scott 1976).

Both velocity components are taken as zero on the lower boundary. The lower rigid boundary is chosen, since we assume that a solid nitrogen layer is based on a solid water-ice mantle. The lower rigid boundary is preserved if a slope (and thus latitudinal spreading of the cap) is included in the model. This can be justified by topography on the scale of 0.5-1 km, which was observed by Voyager 2 just to the north of the southern polar cap and thus seems to be natural on the southern polar cap itself. The lack of topography observed on the southern polar cap can be explained by the highly rheological (at Triton's temperatures) and thick nitrogen ice which buries the relief. The underlying relief would not allow nitrogen glaciers to slide.

The topography observed to the north of the southern cap also justifies our choice of about 1 km thick N_2 deposits, since the southern polar cap was seen by Voyager 2 as a smooth feature. A more detailed justification is provided in the work of Brown and Kirk (1994). They calculated the cap thickness for different latitudes, taking into account conduction in Triton's mantle, sublimation (condensation) from the cap's surface and viscous spreading of the cap under its own weight. The initial thickness of nitrogen ice in their numerical model is 100-150 m globally. These values have been adopted using

an analogy with the Saturnian satellite Titan, which was suggested by Cruikshank *et. al.* (1984). Titan is the only body in the outer Solar System, besides Triton and Pluto, known to have nitrogen in its atmosphere. Titan's thick nitrogen atmosphere was detected by Voyager 1 in 1981. From 61 moons detected in the Solar System only four are known to have atmospheres: Io (SO_2), Titan (N_2), Triton (mostly N_2) and, recently, detected by Hubble Space Telescope a tenuous O_2 atmosphere of Europa. Since Titan's mean surface temperature of about 94 K is above the nitrogen boiling temperature ($\approx$77.36 K at P= 1 atm and Titan's atmospheric pressure of $\approx$1.5 bar near the surface does not increase the boiling temperature noticeably), most of Titan's N_2 has been sublimated.

Following Brown and Kirk (1994), we make the assumption that Triton's total mass of solid N_2 has the same ratio to the satellite's mass as it would be on Titan, if all Titan's atmosphere were condensed. Therefore 120 m of solid nitrogen globally on Titan translates into about 80 m globally on Triton, since Titan's radius of $\approx$2575 km is greater than Triton's. Triton could have accumulated even more nitrogen than Titan, because it was formed much farther from the Sun. Nonetheless, being less massive than Titan, Triton may have lost some of its initial nitrogen inventory by hydrodynamic escape or photo ionization. Titan's abundance of nitrogen is $\approx$0.08 of the solar abundance. If the solar abundance of nitrogen (about 1 part in 1000) is assumed on Triton, then it would be equivalent to a solid GLOBAL layer $\approx$1 km thick (Brown and Kirk 1994). This translates into a cap thickness much more than 1 km. We take this value as an upper limit and reduce our considerations here to the lower abundance of N_2 on Triton. A numerical model by Brown and Kirk (1994) uses the thickness of the globally uniform nitrogen layer as an initial condition. Their calculations predict the existence of permanent polar caps up to 1200" m thick at the poles assuming Titan's abundance of nitrogen on Triton. Seasonal condensation (sublimation) on Triton is only about 1 m (Spencer 1990) hence the seasonal layer does not change the permanent caps much. The result of the Brown and Kirk model calculations with the initial global value of 1.50 m is presented in Fig. 1.

NUMERICAL ANALYSIS

We consider the complete 2D Boussinesq formulation of the problem, rather than

using a parameterized approach based on the Nusselt Rayleigh number relation with the 1/3 power law applicable only in a 1 1) case. (Note that the Nusselt number is the ratio of the conductive plus convective heat flow to the heat flow in the case without convection). Application of this expression for the Nusselt number is common in planetary science but for the purposes of determining the depth of an isotherm having a certain temperature difference with the surface temperature at least a 2D formulation is required. A numerical approach enables us to compute the redistribution of the subsurface temperatures due to convection. The increase of the heat flow in the region of upwelling subsurface currents depends upon the intensity of thermal convection, i. e. upon the Rayleigh number.

We use the Boussinesq approximation to the Navier-Stokes equations for the mathematical description of the problem. The following conditions (Jarvis and McKenzie 1980) for the application are satisfied:

$$\alpha T \ll 1, \quad d/H_T \approx 10^{-3} \ll 1,$$

where T is the absolute temperature, α is the volumetric thermal expansion coefficient, $H_T = c/g\alpha$ is the temperature scale height, c is the specific heat at constant pressure, g is the gravity acceleration, and the thickness d of the convecting layer is taken here as 1 km.

Schluter *et al.* (1965) performed the stability analysis of the Boussinesq equations in the domain of infinite horizontal extent. For the finite high aspect-ratio domains 2D convection at infinite Pr numbers ($Pr = \nu/k$, where η is the kinematic viscosity, $k = \lambda/c\rho$ is the thermal diffusivity λ is the thermal conductivity and ρ is the density). Convection can become time-dependent at Ra about 40 to 50 times critical (see Hansen *et al.* p. 71, 1991 for ref.). This value of Ra is far above our estimates for Triton. Therefore for a constant kinematic viscosity ν we deal numerically with the following non-linear system of the second-order equations in partial derivatives (Landay and Lifshitz 1989):

$$\partial V/\partial t + (VV)V - \nu div \nabla V + \frac{\nabla P}{\rho_0} = -\alpha\theta g, \tag{1}$$

$$div V(x,y) = 0, \tag{2}$$

$$\rho_0 c\partial\theta/\partial t - div(\lambda\nabla\theta) + \rho_0 cV \bullet \nabla\theta + \rho_0 cV \bullet \nabla T_c = 0, \qquad (3)$$

where $T = T_c + \theta$, T_c is the conductive reference temperature, θ is the perturbation over this conductive temperature, p is the perturbation over hydrostatic pressure, g is the gravity acceleration vector. The coefficients c and λ are taken as constants equal to their values at the mean of the upper and lower boundary temperature. Viscous dissipation is neglected in the energy eq. 3. We consider untilted cells only, i.e. the right-hand side in the second scalar eq. 1 is equal to zero. The condition of incompressibility (2) means that the pressure is varying only slightly, so that the density changes due to changes in pressure may be neglected. In eqs. 1-3 density is considered constant (ρ_0) and also taken at the average temperature everywhere, except that in the buoyancy force (right-hand side of eq. 1) where it depends upon temperature. In general, T_c should be taken as a solution of the heat conduction equation with variable coefficients. But for the constant thermal conductivity, the reference temperature can be taken as one-dimensional:

$$T_c = T_{up} - T_{lo})/2 - (T_{lo} - T_{up}) \times y/d,$$

where T_{up}, T_{lo} are temperatures at the upper and the lower boundaries, respectively, and the beginning of the coordinate system is at the center of the domain. For a steady flow which we will consider, time derivatives in eqs. 1-3 are equal to zero.

A constant kinematic viscosity ν is taken in eqs. 1-3 as: $\nu = \eta/\rho_0$, where η is the constant dynamic viscosity at the average of the upper and lower boundary temperatures. This choice of constant internal viscosity is commonly justified in the literature by Booker's experiments 1976 with polybutene oil. It was shown by these experiments that convective heat transport with a variable viscosity can be approximated by a constant viscosity case with the viscosity chosen as mentioned above.

We solved the eqs. 1-3 with the following boundary conditions:

$$V_x(x, d/2) = 0, \qquad V_y(x, d/2) = 0,$$

$$V_y(x,0,t) = 0, \qquad \left.\frac{\partial V_x}{\partial y}\right|_{y=0} = 0,$$

$$\left.\frac{\partial V_y}{\partial x}\right|_{x=0} = 0, \qquad V_x(0,y,t) = 0,$$

$$\left.\frac{\partial V_y}{\partial x}\right|_{x=d_1} = 0, \qquad V_x(d_1,y,t) = 0.$$

For the perturbation temperature, the boundary conditions are:

$$\left.\frac{\partial \theta}{\partial x}\right|_{x=0} = \left.\frac{\partial \theta}{\partial x}\right|_{x=d_1} = 0, \qquad \theta(x,d,t) = 0, \qquad \theta(x,0,t) = 0.$$

The choice of the boundary conditions was justified while developing the physical model.

Following Kirk (1990 and pers. comm.) we consider Nabarro Herring (volume) diffusion as the prevailing creep mechanism in a N_2 ice cap on Triton for plausible solid nitrogen grain sizes and Triton's temperatures. The temperature has to be representative of the whole N_2 layer, therefore we adopt a mean value of 50.5 K for the temperature difference of 25 K across the layer, and 45.5 K for the difference of 15 K. Self-diffusion is a common phenomenon in solids, at least in the vicinity of their melting points (Esteve and Sullivan 1981). It is a thermally activated process. We calculated the nitrogen dynamic viscosity using the self-diffusion coefficient for solid nitrogen molecules from the nuclear magnetic resonance experimental measurements by Esteve and Sullivan (1981):

$$D(T) = 16^{+13}_{-5} \times 10^{-8} \times exp(-(1030 \pm 25)/T), \quad m^2/s. \tag{4}$$

The uncertainty in the exponent stems from the accuracy in determining the activation enthalpy $\Delta H^*/k_B = 1030 \pm 25$ K, where $k_B = 1.381 \times 10^{-23}$ J/K is Boltzmann's constant. We used this coefficient in the dynamic viscosity formula for polycrystalline solids with volume diffusion (Raj and Ashby 1971):

$$\eta(T) = \frac{C d_g^2 k_B T}{42 D(T) \Omega}, \tag{5}$$

where $\Omega = 4.7 \times 10^{-29} m^3$ is the molecular volume (Eluszkiewicz 1991), d_g is the grain diameter (assuming spherical grains), and C is the numerical correction factor for finite strains which reflects the changes of the grain's shape. The factor C is roughly 0.4 (Kirk 1990; Raj and Ashby 1971; Goodman *et al.* p. 272, 1981). Thus the main uncertainty in these calculations is the mean grain size of nitrogen deposits on Triton.

According to eq. 5, the maximum viscosity variation across all of Triton's solid nitrogen layer is about 2.83×10^4 for the temperature variation of 25 K. Torrance and Turcotte (1971) reported as a result of their numerical experiments that the Nu number is approximately constant (i.e. there is almost no change in heat transport between the horizontal boundaries) if the viscosity contrast across a layer is more than 20 and less than 2.2×10^4. In their computations $Ra/Ra_{critical} = 5.475$ for free-free boundaries and an infinite Prandtl number.

Even a small decrease in the average grain size gives a significant rise to the ratio $Ra/Ra_{critical}$, where the Rayleigh number is defined as $Ra = \alpha g \Delta T d^3 / \nu k$. Thermophysical coefficients are taken in this definition at the average of the upper and lower boundary temperature, ΔT is the temperature difference between its value at the lower and the upper boundaries and $Ra_{critical} = 1100.65$ (Chandrasekhar 1981). This number is the minimum Rayleigh number required for the onset of convection for upper stress-free and lower rigid boundary conditions. The minimum is taken with respect to till horizontal wavenumbers. The critical Ra provides a sufficient condition for the onset convection in an untilted domain. The corresponding horizontal wavenumber is 2.682. Both critical values are independent of the Prandtl number. Representing the system in a dimensionless form yields a product of the Pr^{-1} (reciprocal of Prandtl number) and the sum of the acceleration term $\partial V / \partial t$ and the inertial term $(V \nabla) V$. The Prandtl number for the solid nitrogen on Triton, evaluated at the mean of the upper and lower boundary temperatures, is essentially infinite (Table 1). Hence the above-mentioned product can be omitted.

The steady-state solution of the eqs. 1-3 is not unique, if the horizontal wavenumber of the convective cell is not specified. There is no way of determining the horizontal wavenumber a for the initial temperature and the for the velocity perturbation over the conductive state in Triton's nitrogen polar caps. (Here we additionally assume uniform

cells and thus have only one horizontal wavenumber). This wavenumber determines the width of the formed cells (π/a) in the case of a layer with infinite horizontal extent, and therefore influences the effectiveness of the convective heat transport across the layer, i. e. influences the Nusselt number. For example, the maximum Nusselt number for a fixed value of the Rayleigh number (and therefore the most effective heat transport across the layer), is reached at an aspect ratio of the cell equal to one in the case of free-free boundary conditions (Turcotte and Schubert 1982). Extreme initial horizontal wavenumbers provide minimum and maximum Nusselt numbers for a given Ra. Horizontal wavenumbers a for stable 2D cells are known to be in the interval 1.8 - 4.3 for free-rigid boundaries (Fig. 2). For a 1 km solid nitrogen layer we obtain the range of cell widths $l = a/\pi$: 0.57 - 1.4 km. And the maximum width of a stable roll is much less than the satellite's mean radius of about 1352 km. This means that sphericity of the domain can be neglected when we take a narrow cross-section in the subsurface.

The conventional criterion used to select a wavenumber was based for a long time on a hypothesis (Malkus 1954) that the convecting fluid should transport a maximum amount of heat (thus maximizing the Nusselt number). This may be correct for the turbulent regime under high Rayleigh numbers, but was shown numerically to be incorrect (Foster 1969) for the two-dimensional laminar convection under infinite Prandtl number, which is likely to take place in Triton's polar caps. In the case of a domain with infinite horizontal extent, the convective solution is defined by the set (Ra, Pr, a). These values are not completely independent, since under high Rayleigh numbers the growth of Ra influences the horizontal wavenumber a. Unfortunately, theoretical and experimental works report the opposite influence (see Booker 1976 for references). For a finite domain, not only the initial wavenumber a influences the size and number of formed convective cells but the aspect ratio of the domain as well (Foster 1969). An example can be given for a domain with an aspect ratio much greater than one, where one initially introduced cell breaks into two cells (McKenzie *et al.* 1974). The effect of the lateral boundaries is to put a constraint on the allowable motion, thus this constraint may cause lowering of the Nusselt number. This was also confirmed by Foster's (1969) computations.

We took an initial temperature field in our computations as a bilinear interpolation of

the solution for temperature from Kvernvold (1979) with $Ra = 5 \times Ra_{critical}$. Analysis is performed there for the layer of an infinite horizontal extent having a horizontal wavenumber of 2.6. Hence an aspect ratio of the cell (and thus of our domain, since we consider only one cell) is $\pi/a \approx 1.21$. The chosen wavenumber is close to the wavenumber 2.682 (Chandrasekhar 1981) corresponding to the minimum critical Rayleigh number for our free-rigid boundaries. Therefore, it provides the stability condition for the two-dimensional rolls in a wide range of Ra numbers: from Ra slightly higher than $Ra_{critical} = 1100.65$ up to Ra $\approx 32 \times Ra_{critical}$ (Fig. 2). If the solid-nitrogen grains on Triton are much smaller than we consider in this work, the Rayleigh numbers may exceed the second critical Ra $\approx 47 \times Ra_{critical}$ for the stable rolls, implying time-dependence in convective currents.

We constructed a finite-difference scheme in which the convective term in the energy eq. 3 is treated using an upwind technique and all other spatial derivatives are approximated with the central space differences. The scheme has a 1st order of approximation in spatial variables for a non-uniform grid. The non-uniformity is needed to resolve the boundary layers. An iterative method is used to solve the resulting non-linear system of discrete equations. For the case without time-dependence, relaxation of the solution of the fully implicit scheme to the stationary solution was achieved. In our calculations of the conductive-convective temperatures and of the corresponding velocity fields, nitrogen thermophysical coefficients (Scott 1976) were considered to be constant and taken as indicated in Table 1.

RESULTS

Nitrogen vapor pressure is extremely sensitive to temperature changes at Triton's and Pluto's cryogenic temperatures. A temperature rise of 1 K over the surface value is enough to double the nitrogen vapor pressure. In turn, this increase in pressure is sufficient to drive Triton's plumes at the initial supersonic speed of about 125 m/s (Yelle *et al.* 1991). Taking the negative influence of atmospheric drag and the positive influence of plume buoyancy into consideration, it was calculated by Yelle *et al.* (1991) that the indicated initial speed can bring the plumes to the observed height of about 8 km. For the solid-nitrogen convective cell we computed that the isotherm T_{up}+1 K rises on the ascending

side of the convective cell to a depth of ≈16.4 m (the closest approach of this isotherm to the surface) for $Ra = 5 \times Ra_{critical}$ (see Fig. 3 for illustration). This value is less than the corresponding depth of 40 m for the pure conductive case having the same constant temperature gradient of 25 K/km. Thus, existence of stable subsurface vents exposing warmer by 1 K N_2 ice to Tritonian atmosphere is much more probable for the case with convection. The indicated temperature increase will be even closer to the surface for the larger Rayleigh numbers. Analyzing the structure of the computed temperature field we see that the conductive-convective temperature gradient can be considered approximately constant in the upper boundary layer. We showed that, if convection even with small supercritical Ra numbers occurs, it may drive the plumes by redistributing internal heat in the subsurface without the solid-state greenhouse effect. Subsurface thermal convection redistributes the internal heat flow in a way that the heat flow is increased in the vicinity of an upwelling subsurface plume (left side of the convective cell in Fig. 4) and is decreased in the region of downwelling currents, compared to a pure conductive case. Therefore, atmospheric plumes can be considered a manifestation of subsurface convective plumes.

Laminar convection in solid nitrogen occurs if a nitrogen ice layer is thick enough and N_2 ice grains are small enough. We computed an approximate critical thickness of the nitrogen layer belonging to different plausible polar caps. This thickness is presented in Fig. 5A as a function of N_2 ice average grain diameter and is sufficient to obtain $Ra = Ra_{critical}$ and $Ra = 5 \times Ra_{critical}$, respectively. For the higher pair of curves the self-diffusion coefficient of nitrogen ice is assumed to be equal to the average estimate from the measurements of Esteve and Sullivan (1981), whereas for the lower pair, the self-diffusion coefficient is taken at the upper limit from the same experimental measurements (eq. 4). In our computations of the Rayleigh numbers we take into consideration the change of the mean temperature (at which the parameters comprising the Ra are taken) with the change in the nitrogen thickness. The seventh-order polynomial was used to approximate the temperature dependence of density, the second-order polynomials for the heat resistivity (the inverse of the heat conductivity), and the third and second-order polynomials for the temperature dependence of the N_β heat capacity, respectively. A pure conductive temperature gradient of 25 K/km is assumed. This gives the maximum

thickness of about 1 1 1 1 1 for the case without melting at the base. Fig. 5B is a blowup of Fig. 5A for small thicknesses. It demonstrates that convection onsets for arbitrary thin layers if solid nitrogen grain diameters are less than the certain critical values. For example, for the layer 33.33 m thick the critical diameter is calculated to be about 0.064 μm using the average estimate for the self-diffusion coefficient from eq. 4, and it is about 0.12 μm using the upper limit of the measurements of the self-diffusion coefficient and the pure conductive gradient of 25 K/km. The corresponding diameters for the onset of the solid-state convection in a layer 11 m thick, when the conductive gradient of 22.5 K/km is assumed, are about 0.6×10^{-8} m and 0.1122×10^{-7} m. Note that the critical thickness is a very sensitive function of a solid N_2 grain size, which is an unknown parameter for Triton. In Fig. 5C the same set of curves is plotted as in Fig. 5A but the pure conductive gradient is assumed to be 22.5 K/km. The corresponding grain diameters are larger in this case compared to the conductive gradient of 25 K/km.

It is highly plausible that a shallow vent (in a region of the upwelling subsurface plume) needed for a geyser to operate is maintained by multiple cubic-hexagonal phase transitions in solid nitrogen (Duxbury and Brown 1993). These phase transitions were observed in laboratory experiments to be disruptive (Scott 1976), at least going from the higher temperature hexagonal phase to the denser cubic phase of nitrogen. Numerical modeling (Duxbury and Brown 1993) showed that α - β nitrogen fronts can penetrate down to about 35 m for solid N_2 layers thicker than 150 m, often with two phase fronts propagating simultaneously. In the presented subsurface convective model the viscous spreading of the cap under its own weight was not taken into account, since only untilted convective cells were considered.

Addressing the question of impurities, we note that CH_4, CO and CO_2 as minor constituents in the solid solution with N_2, can raise the phase transition temperature between the cubic α and hexagonal β crystalline phases. When the surface temperature decreases, this can cause the earlier shattering of the more contaminated areas (Duxbury and Brown 1993). Viscous spreading of the solid-nitrogen cap under its own weight may be responsible for closing the geyser's vent and stopping the eruption.

DISCUSSION AND FUTURE WORK

Though the requirements on the thickness of the nitrogen layer and the corresponding grain size seem to be strict, we have to keep in mind that in reality there is a slope present. For this case convection onsets for $Ra < Ra_{critical} = 1100.65$. because of the virtual increase of the effective height of a convective cell. Thus convection occurs for the layers whose thickness is smaller than we have calculated considering only the *sufficient* conditions for convection. Therefore in reality convective conditions on Triton are *lessrigorous* than we have presented on Figs. 5. A tilted cell can be considered also in a 2D approximation but periodic boundary conditions for the velocity on lateral boundaries are more appropriate in this case. Eqs. 1-3 do not depend upon the choice of a coordinate system. For the more general case of a tilted convective cell, it is convenient to choose the OX axis along the slope and OY perpendicular to it. If the angle between OX and the horizontal is equal to γ, then the gravity acceleration vector $g = \{gsin\gamma, gcos\gamma\}$ in the chosen coordinate system. We estimated the maximum slope (near the edge of the cap) to have $sin\gamma = 10^{-6}$, which is much less than the critical value of about 5 deg, when convection changes to a 3D mode (Kassemi, pers. com.) We compared the average horizontal velocity component in the absence of the slope in our conductive-convective model calculations with the along-the-slope velocity component from Brown and Kirk (1994) in the absence of thermal convection. Both values are about 3 mm/Earth yr. Therefore further numerical simulations, allowing coupled convection and viscous spreading are needed.

Since our model works for sufficiently thick N_2 layers, one would expect to find geysers near the South Pole as well. Visual images taken by the Voyager 2 had their best resolution of $\approx$1 km near the terminator (45 deg N), and their worst resolution was near the South Pole. Moreover, the South Pole was viewed at oblique viewing angles. Thirdly, the stereo images, where the plumes were originally detected, were taken only of a few regions on Triton. Therefore Voyager 2 images cannot supply us with sufficient information about the polar regions.

We solved eqs. 1-3 numerically for a constant viscosity. In the case of a strongly temperature-dependent viscosity, a nearly stagnant region develops near the upper boundary. Therefore, an effective height of the convective cell is reduced. The heat transport in this overlayer is primarily by conduction (isotherms are almost parallel). Since the thermal

conductivity of solid nitrogen is very low (Table 1), scaling conducting overlayer shields the deeper convecting layers from the outer cooling. This prevents viscosity beneath the overlayer from increasing and hence prevents convection in the underlayers from cessation. Thus we do not expect the conducting upper layer to be thick compared to the thickness of the whole N_2 cap. Future numerical modeling with variable viscosity for solid nitrogen is needed to determine the closest approach to the surface of T_{up} + 1 K isotherm. Large scale modeling will also be useful since it includes horizontal interactions between convective cells.

Since dust is present in the cap, dust particles are restricting the growth of solid nitrogen crystals. The growth of crystals is caused by surface tension. Change in the orientation of grain boundaries, which occurs during the growth, may cause the cessation of the growth even in a pure substance. One can apply the Zener theory for the estimate of the grain size of solid nitrogen (Kirk, pers. comm.). The theory was suggested for the grain growth in metals and was considered only semiquantitative (Smith 1948). It estimates the maximum grain size depending upon the size of inclusions, since there are other factors which can stop the grain growth. Among those are changes in the orientation of the grain boundaries during the growth, different shapes of inclusions, the positioning of inclusions at grain and edges vertices. Moreover, there is a feedback from the thickness of the whole layer on the size of grains comprising the layer (experiments with metals, Smith 1948 p. 48). Following Kirk (a letter to N. S. Duxbury dated March 31, 1995) in calculations of N_2 frost mass flux, we get a value of $3.17 \times 10^{-8} kg/m^2 s$. In these calculations the solar flux on Triton was taken from Brown *et al.* (1991) and the long-term average value was used. Then, using the dust flux value of $4.5 \times 10^{-15} kg/m^2 s$ and the dust grain diameter estimate of $\approx 5. \times 10^{-7}$ m from Pollack *et al.* (1990), we obtain a maximum solid nitrogen grain diameter as ≈ 10.5 cm. Though the optical estimates of a mean dust grain diameter were good, the obtained upper limit for solid N_2 grain diameter in Triton's permanent nitrogen layer has an uncertainty of about a factor of ten. It stems from the uncertainty in the dust flux estimates obtained by Pollack *et al.* (1990) using Voyager 2 data.

SUMMARY

Our numerical simulations of convection in solid nitrogen showed that the temperature difference of 1 K can be reached in the case of conductive-convective heat and mass transport much closer to the surface than in the pure conductive case. We assumed that Triton is completely differentiated with a core being ≈ 70 % of the satellite's mass. (This estimate stems from the $\rho = 2.054 g/cm^3$, Voyager 2 observations in August 1989). The corresponding internal heat flow at the surface is $\approx 3.1 \times 10^{-3} W/m^2$ (Smith *et al.* 1989). Due to the small thermal conductivity of solid nitrogen this translates into a large thermal gradient of 15 - 30 K/km in N_2 ice. The temperature difference of 1 K is enough to double the N_2 vapor pressure and thus to drive the plumes to the observed height of about 8 km. Subsurface vents to a depth where $\Delta T = 1$ K can be provided by shattering of solid nitrogen as a result of the crystalline phase transition (Duxbury and Brown 1993).

REFERENCES

Booker, J. R. 1976. Thermal convection with strongly temperature dependent viscosity. *J. Fluid Mechanics* **76**, 741-754.

Brown, R. 11., R. L. Kirk, T. J. Johnson, and 1,. A. Soderblom 1990. Energy sources for Triton's geyser-like plumes. *Science* 250, 431-434.

Brown, R. H., 'J. v. Johnson, J. 1). Goguen, G. Schubert, and M. N. Ross 1991 . Triton's global heat buc lget. *Science* 251 , 1465-1467.

Brown, R. H., and R. L. Kirk 1994. Coupling of volatile transport and internal heat flow on Triton, *J. Geophys. Res.*, *99*, No. E1, 1965-1981.

Chandrasekhar, S. 1981. Hydrodynamic and Hydromagnetic Stability, Dover, New York.

Christensen, U. R. 1984. Convection with pressure- and temperature-dependent non-Newtonian rheology, *Geophys. J. R. Astr. Soc.*, *77*, 343-384.

Christensen, U. R. 1984. Heat transport by variable viscosity convection and implications for the Earth's thermal evolution, *Physics of the Earth and Planetary Interiors*, **35**, 264-282.

Cruikshank, D. P., T. L. Roush, T. C. Owen, Geballe, T. R., C. de Bergh, B. Schmitt, R. H. Brown, and M. J. Bartholemew 1993. Ices on the surface of Triton. *Science*, **261**, 742-745.

Duxbury, N. **s.,** and R. H. Brown 1993_a. The phase composition of Triton's polar caps. *Science* **261**, *748-151.*

Duxbury, N. s., and R. H. Brown 1993_b. Solid-st ate convection in Triton's polar caps. *Bull. Am. Astron. Soc. 25* **No3**, *1111-1112.*

Duxbury, N. S., and R. }1. Brown (1 992). Thermal evolution of Triton's nitrogen layer. *Bull. Am. Astron. Soc. 24* **No3**, 966.

Eluszkiewicz, J. A. 1991. On the microphysical state of the surface of Triton. J. G. R. 96, 19217-19229.

Esteve, D., and N. S. Sullivan 1981. N.M.R. study of self-diffusion in solid N_2.
Solid State Communications **39**, 969-971.

Foster T. D. 1969. The effect of initial conditions and lateral boundaries on convection. *J. Fluid Mechanics*, 37, 81-94.

Goldsby D. L., D. L. Kohlstedt. 1995. The transition from dislocation to diffusion creep in ice. *LPSCXXVI*, **1**, 473-414.

Hansen, C. J., and D. A. Paige 1992. A thermal model for seasonal nitrogen cycle on Triton. *Icarus*, **99**, 273-288.

Hansen, U., D. A. Yuen, and S. E. Kroening 1992. Mass and heat transport in strongly time-dependent thermal convection at infinite Prandtl number.
Geophys. Astrophys. Fluid Dynamics, **63**, 67-89.

Jarvis, G. T., and D. P. McKenzie 1980. Convection in a compressible fluid with infinite Prandtl number. *J. Fluid Mechanics*, *96, part 3*, 515-583.

Kirk, R. L., R. H. Brown, and L. A. Soderblom 1990. Subsurface energy storage and transport for solar-powered geysers on Triton. *Science* **250**, 424-428.

Kirk, R. L. 1990. Diffusion kinetics of solid methane and nitrogen: Implications for Triton. *LPSCXXI*, 631-632.

Klinger, J. 1980. Influence of a phase transition of ice on the heat and mass balance of comets. *Science* 209, 634-641.

Kvernvold, O. 1979. Rayleigh-Benard convection with one free and one rigid boundary, *Geophys. Astrophys. Fluid Dynamics*, **12**, 273-294.

Landay, L. D., and E. M. Lifshitz 1989. *Fluid mechanics*, Pergamon Press, 217-225

Malkus, W. V. R. 1954. The heat transport and spectrum of thermal turbulence.
Proc. Royal Soc., ***A*** *225*, 196.

McKenzie D. P., J. M. Roberts, and N. O. Weiss 1974. Convection in the earth's mantle: towards a numerical simulation. *J. Fluid Mechanics* **62**, **3**, 465-538.

Paterson, w. S.B. 19s1 . *The Physics of Glaciers*. Pergamon 1'1'('ss.

Pollack, J. B., J. M. Schwartz, and Ii. Rages 1990. Scat terers in Trit on's atmosphere: implications for the seasonal volatile cycle, *Science* 250, 440-443.

Raj, R., and M. F. Ashby 1971. On grain boundary sliding and diffusional creep, *Metallurgical Transactions* **2**, 1113-1127.

Schluter, A., D. Lortz, and F. Busse 1965. On the stability of steady finite amplitude convection. *J. Fluid Mechanics* **23**, 129-144.

Scott, T. A. 1976. Solid and liquid nitrogen. *Physics Reports* **27**, 89-157.

Smith, B. A., 1,. A. Soderblom, and 63 co-authors 1989. Voyager 2 at Neptune: Imaging Science Results. *Science 246, 142? -1449,*

Soderblom 1,. A., S. W. Kieffer, T. 1,. Becker, R. 11. Brown, A. F. Cook, C. J. Hansen, T. V. Johnson, R. L. Kirk, E. M. Shoemaker 1990. Triton's p;(ysrr-like plumes: discovery and basic characterization. *Science* **250**, **410 41[).**

Spencer, J. 1{. 1990. Nitrogen frost migration on Triton: A historical model. Geophys. Res. Lett. 17, 1769 1772.

Spencer, J. R. and J. M. Moore 1992. The influence of thermal inertia on temperatures and frost stability on Triton. *Icarus* **99**, 261-272.

Torrance, K. E., and D. L. Turcotte 1971. Thermal convection with large viscosity variations. *J. Fluid Mechanics*, **47**, 113-125.

Tryka, K. A., R. H. Brown, V. Anicich, D. P. Cruikshank, and T. C. Owen 1993. Spectroscopic determination of the phase composition and temperature of nitrogen ice on Triton. *Science*, **261**, 751-754.

Tryka, K. A., R. H. Brown, D. P. Cruikshank, T. C. Owen, and T. R. Geballe 1994. The temperature of nitrogen ice on Pluto and its implications for flux measurements. *Icarus*, **112**, 513-527.

Turcotte, D. L., and G. Schubert 1982. *Geodynamics*, Wiley, New York.

Yelle, R. V., J. I. Lunine, and D. M. Hunten 1991. Energy balance and plume dynamics in Triton's lower atmosphere, *Icarus*, **89**, 347 -358.

ACKNOWLEDGMENTS

The authors are very grateful to E. R. Ivins (JPL), M. Kasseni (JPL), R. L. Kirk (USGS) and J. A. Stansberry (Lowell Observatory) for the useful discussions and C. H. Acton (JPL) for reading the early versions of the manuscript.

Figure Captions

Fig. 1. Possible nitrogen cap thickness versus latitude. Computations were taken from the Brown and Kirk (1994) model with an initial globally uniform nitrogen layer 150 m thick.

Fig. 2. Region where 2D convective cells with upper free and lower rigid boundaries are stable relative to arbitrary 3D infinitesimal disturbances. The plot is taken from Kvernvold (1979).

Fig. 3. Rising of the upper 39 K isotherm (solid curve) under the influence of the ascending warm currents of solid nitrogen (left side) and the isotherm lowering on the right side of the convective cell due to the descending cold currents. A surface temperature of 38 K and $Ra = 5 \times Ra_{critical}$ are assumed. For comparison, the pure conductive 39 K isotherm, corresponding to the steady-state gradient of 25 K/km, is marked with the upper dashed line. It is located at the depth of 40 m. Similar behavior of the lower (T= 60.5 K) conductive-convective isotherm is shown. It corresponds to the near-melting temperature of solid nitrogen. The corresponding conductive 60.5 K isotherm is marked by the lower dashed line.

Fig. 4. Velocity field computed for a 2D convective cell (roll) with the upper free and lower rigid boundary conditions.

Fig. 5A. Thickness of permanent solid nitrogen layers sufficient to obtain $Ra = Ra_{critical}$ and $Ra = 5 \times Ra_{critical}$ versus a plausible average solid N_2 grain diameter. The first is marked by the curves with filled circles and the second - by the curves with open triangles. The areas above the curves correspond to the cases of $Ra > Ra_{critical}$ and $Ra > 5 \times Ra_{critical}$, respectively. A pure conductive gradient is fixed for all depth at 25 K/km. For the higher pair of curves the self-diffusion coefficient of nitrogen ice is assumed to be equal to the average estimate from the measurements of Esteve and Sullivan (1981). For the lower pair the self-diffusion coefficient is taken at the upper limit from the same experimental measurements (eq. 4).

Fig. 5B. A blowup of Fig. 5A for small thicknesses and the average estimate of the self-diffusion coefficient for solid nitrogen (eq. 4).

Fig. 5C. The same set of curves as in Fig. 5A but the corresponding pure conductive gradient is assumed to be 22.5 K/km.

Table 1.
Convective model parameters.

Temperature', K	***50.5***
Density, $\frac{kg}{m^3}$	***970***
Heat capacity, $\frac{J}{KgK}$	1482,5
Thermal conductivity, $\frac{W}{mK}$	0.207
Thermal diffusivity, $\frac{m^2}{s}$	1.44"10-7
Volumetric thermal expansion coefficient, K^{-1}	$2 \cdot 10^{-3}$
Gravitational acceleration, $\frac{m}{s^2}$	***0.79***
Dynamic viscosity[b], Pas	**2.5469797 "1013**
Kinematic viscosity, $\frac{m^2}{s}$	2.628462 O*1O1O
Prandtl number[b]	$2 \cdot 10^{17}$

[a] Average of the upper and lower boundary temperature for solid N_2.

[b] For solid N_2 grain diameter of 0.2 mm is assumed. Diffusion coefficient from Esteve and Sullivan (1981) is used to calculate the temperature dependence of η and pressure dependence is neglected (P= O),

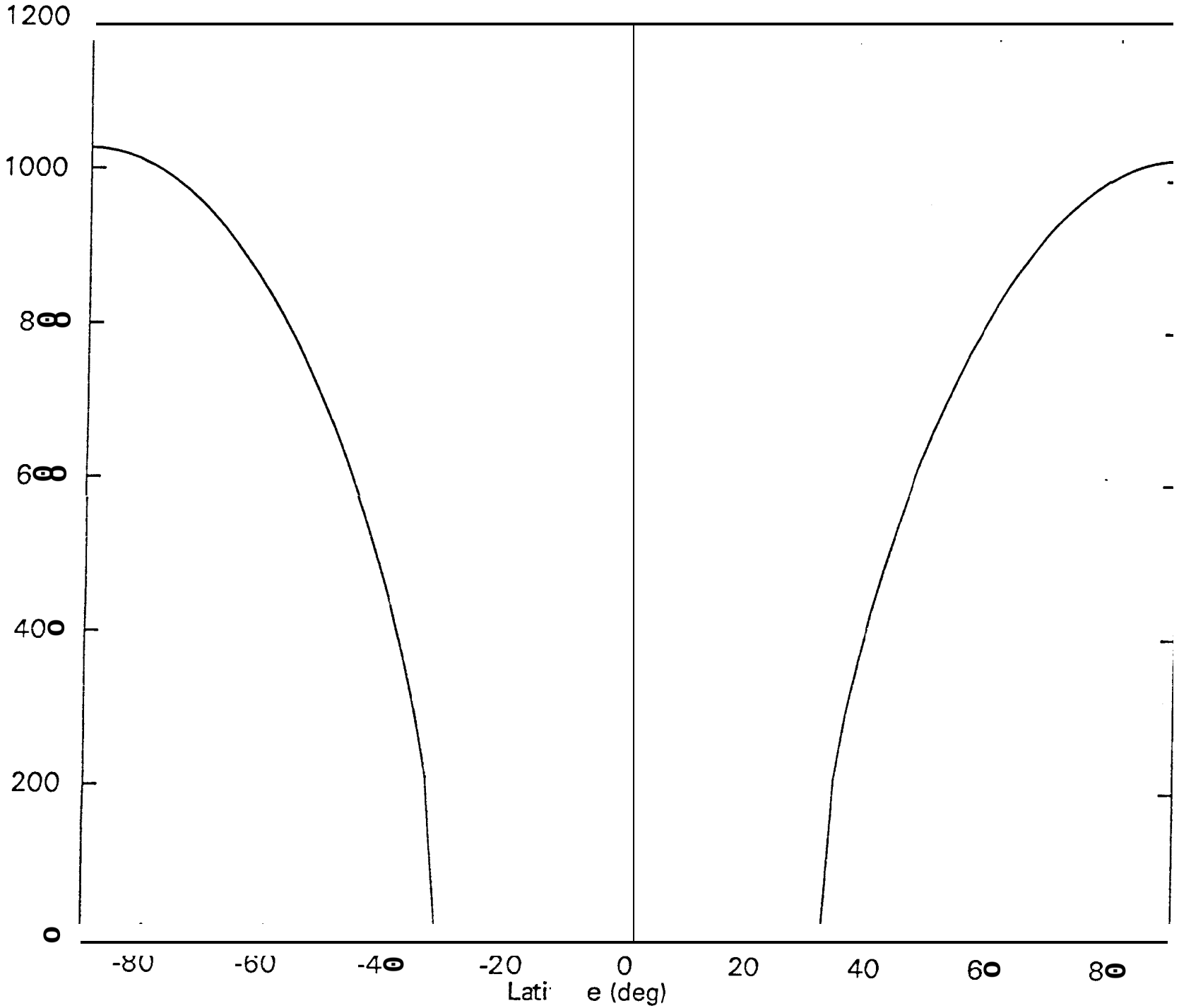
1200
1000
800
600
400
200
0
-80
-60
-40
-20
0
20
40
60
80
Latitude (deg)

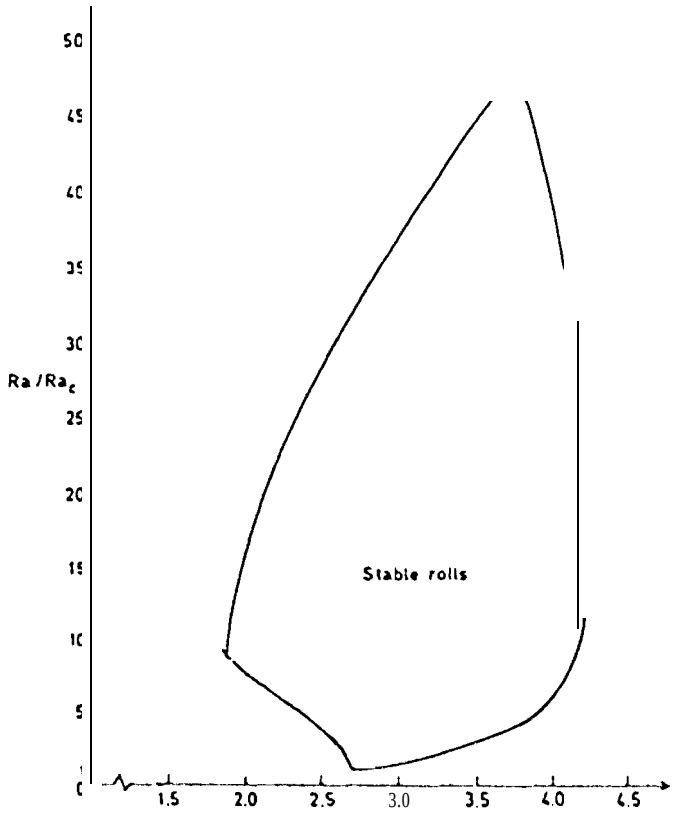
50
45
40
35
30
Ra/Ra$_c$
25
20
15
10
5
0
Stable rolls
1.5
2.0
2.5
3.0
3.5
4.0
4.5
a

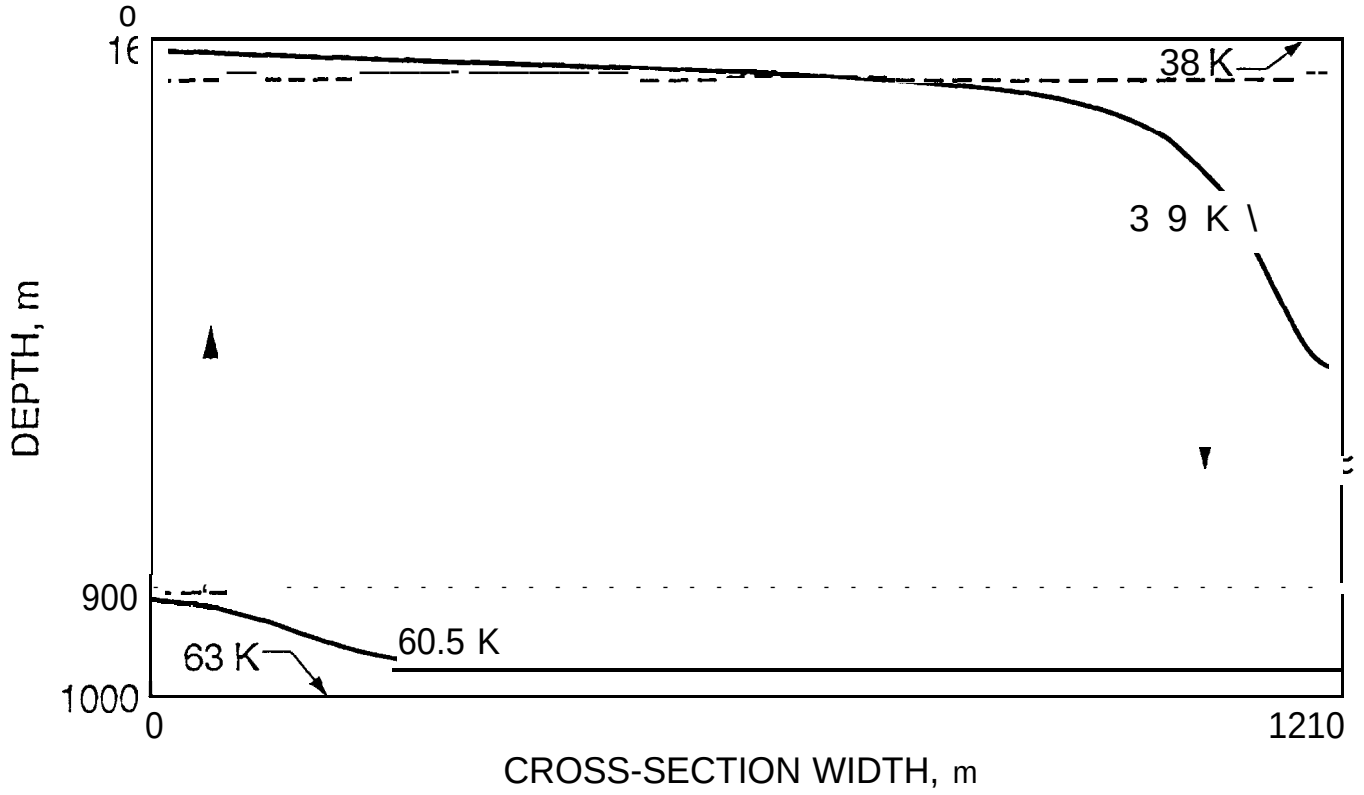

original Fig 3

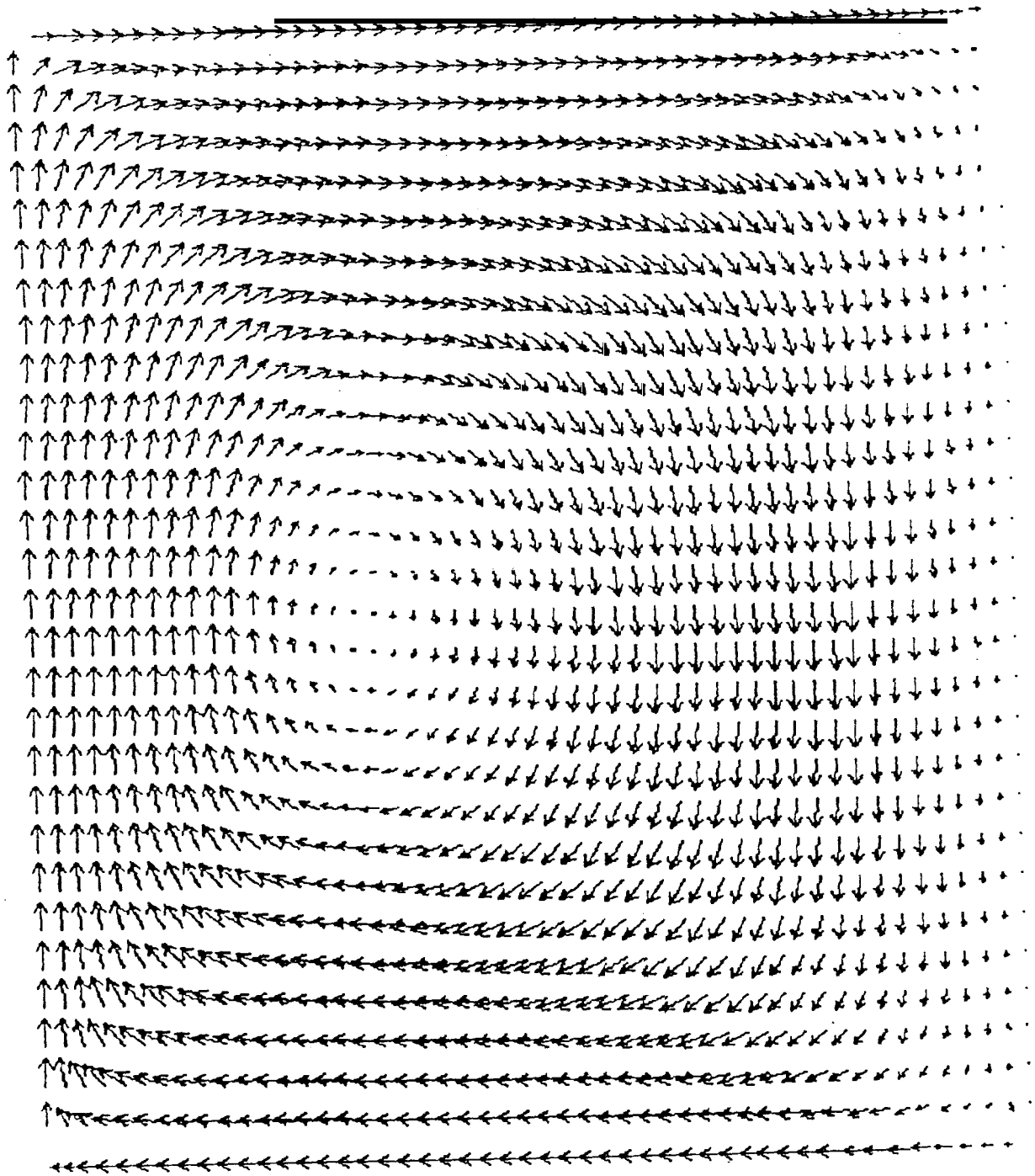

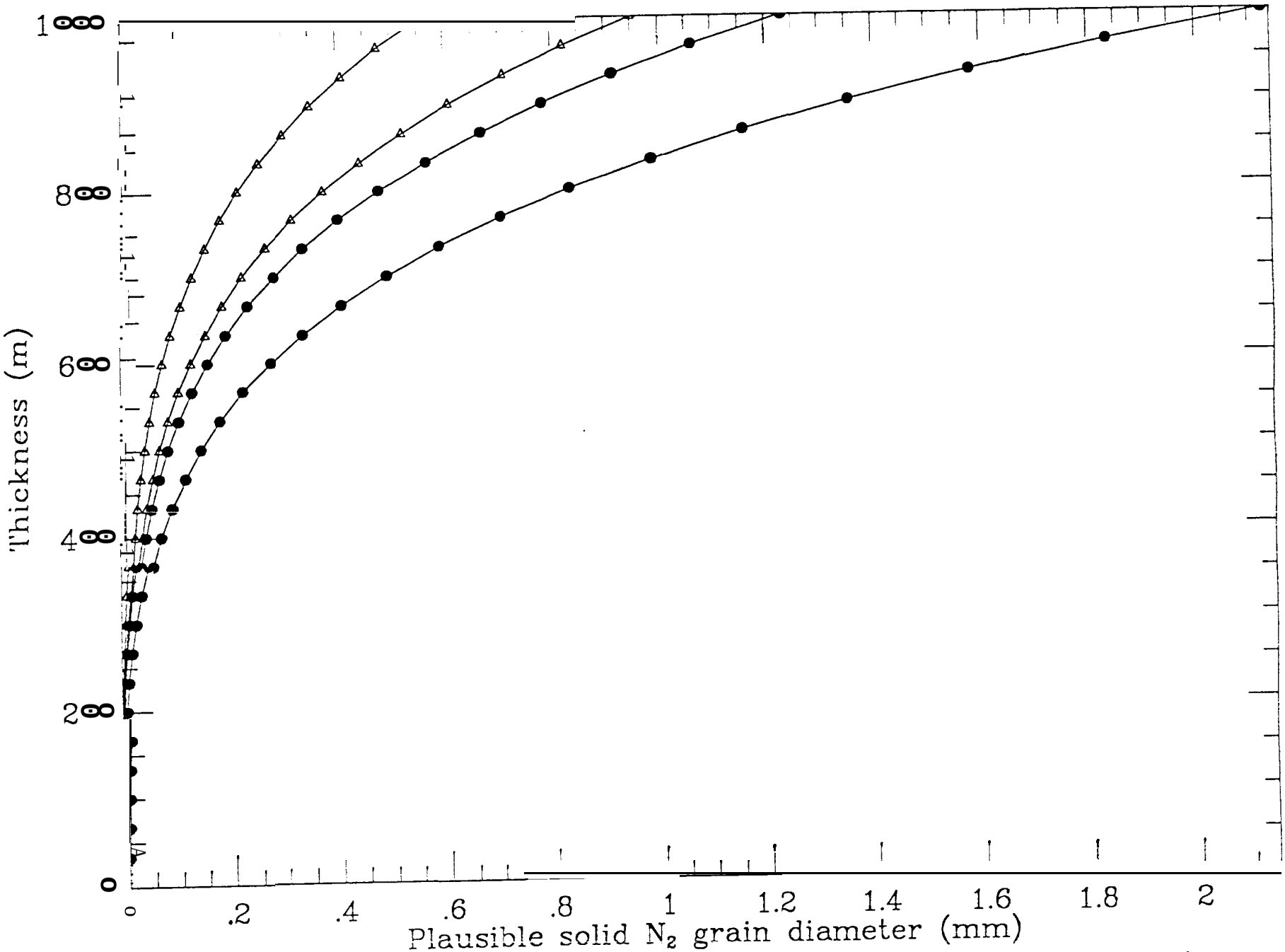
1000
800
600
400
200
0
Thickness (m)
0
.2
.4
.6
.8
1
1.2
1.4
1.6
1.8
2
Plausible solid N_2 grain diameter (mm)

Fig. 4

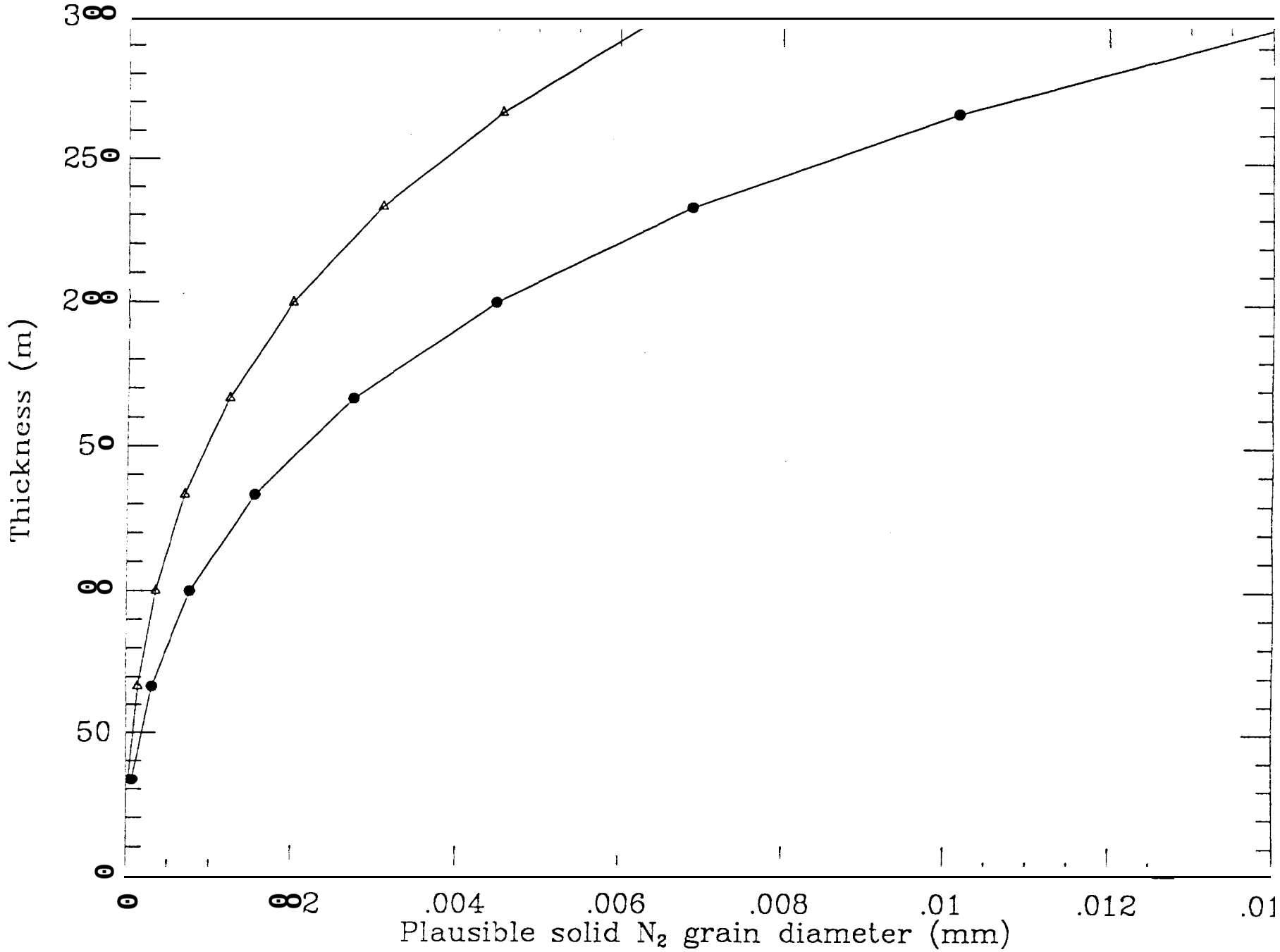

Dieterich and Brown, original Fig 5B

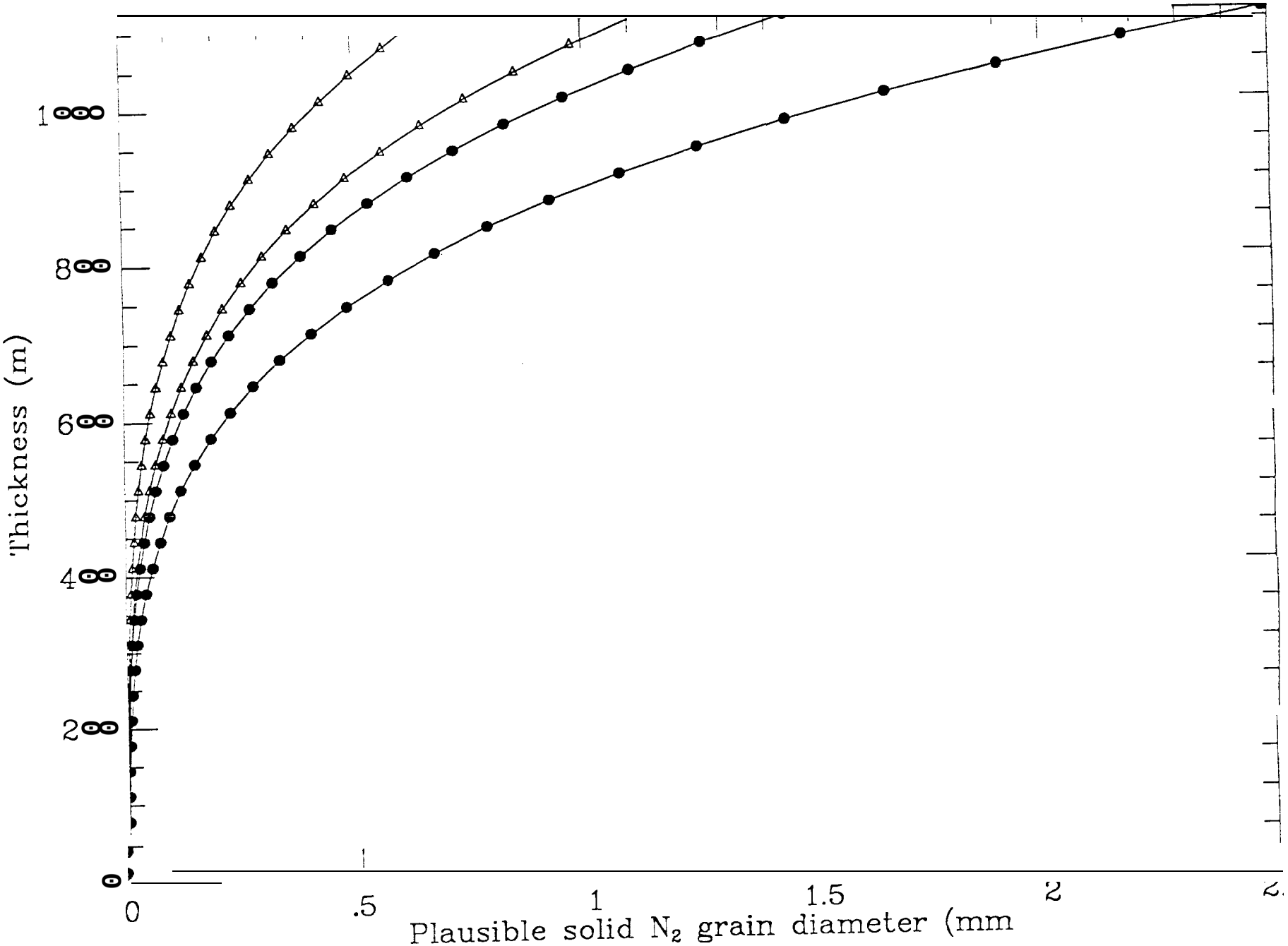
Thickness (m)
1000
800
600
400
200
0
0
.5
1
1.5
2
Plausible solid N_2 grain diameter (mm